Supplementary Information (SI) for Journal of Materials Chemistry C.

Supplementary Information

for

$PtSe_2$ Thickness Engineering Towards Fast Response, Large Linear Dynamic Range, and Broadband $PtSe_2$/Si Heterojunction Photodetector

Ji Zeng[1], Changyong Lan[1, 2*], Yiyang Wei[1], Shuren Zhou[1], Chuanfu Huang[3], Mingyu Xu[1], Yi Yin[1, 2], Chun Li[1, 2]

1. State Key Laboratory of Electronic Thin Films and Integrated Devices, School of Optoelectronic Science and Engineering, University of Electronic Science and Technology of China, Chengdu 610054, China

2. Tianfu Jiangxi Laboratory, Chengdu 641419, China

3. School of Materials Science and Physics, China University of Mining and Technology, Xuzhou, Jiangsu 221116, China

*Corresponding author: cylan@uestc.edu.cn

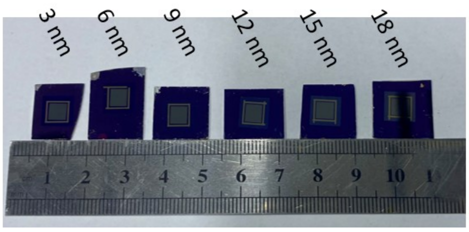

Figure S1. Digital optical images of the devices with various $PtSe_2$ thicknesses.

Determination of the diodes' parameters

The diodes' parameters can be obtained from Cheung's functions [1]:

$$\frac{\mathrm{d}V}{\mathrm{d}\ln I} = IR_{\mathrm{s}} + \frac{nkT}{q} \tag{1}$$

$$H(I) = V - \frac{nkT}{q}\ln\left(\frac{I}{A^{*}ST^{2}}\right) \tag{2}$$

$$H(I) = IR_{\mathrm{s}} + n\Phi_{\mathrm{B}} \tag{3}$$

where R_s is the series resistance, n is the ideality factor, T is the absolute temperature, q is the elementary charge value, A^* is the Richardson constant, Φ_B is the Schottky barrier height. From the dV/dln$I$ – I plots and linear fittings (**Figure S2**), the R_s and n can be evaluated.

Utilizing the obtained n to calculate $H(I)$ according to equation (2), and drawing H versus I plots (**Figure S3**), the Schottky barrier heights can be evaluated.

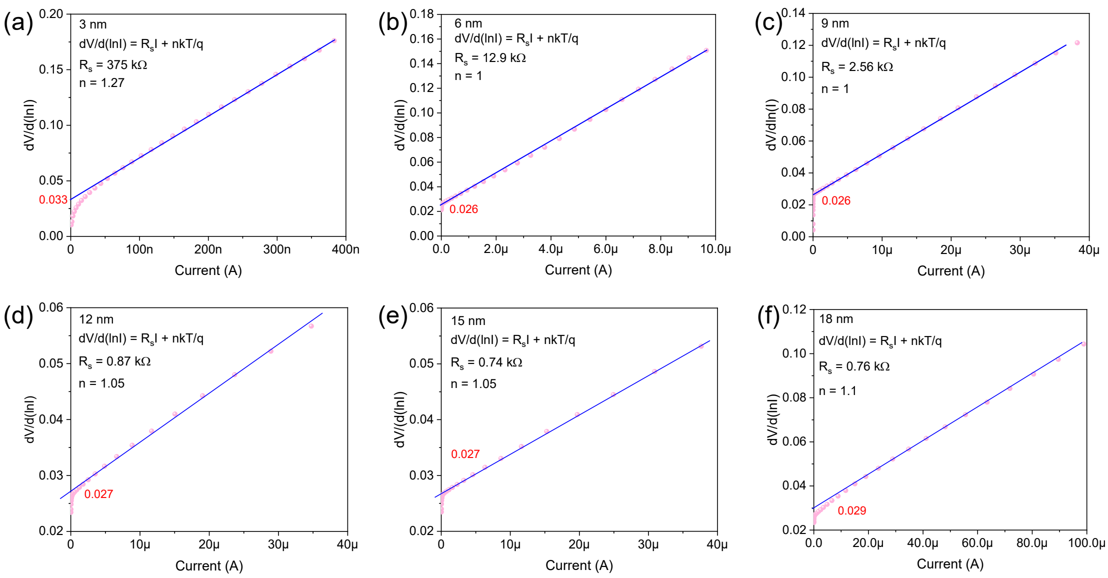

Figure S2. dV/dln$I$ versus I plots to determine n and R_s. (a) 3 nm, (b) 6 nm, (c) 9 nm, (d) 12 nm, (e) 15 nm, (f) 18 nm.

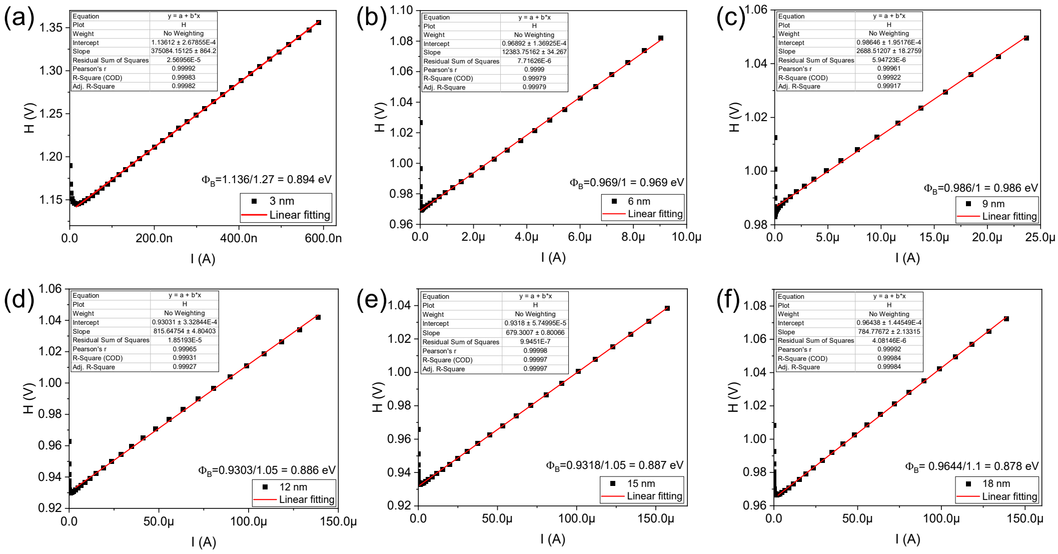

Figure S3. *H* versus *I* plot to determine Φ_B. (a) 3 nm, (b) 6 nm, (c) 9 nm, (d) 12 nm, (e) 15 nm, (f) 18 nm.

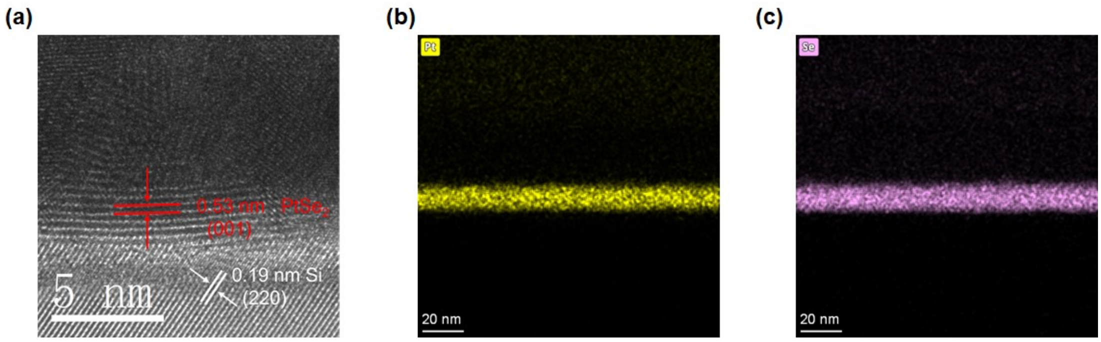

Figure S4. HRTEM and EDS mapping. (a) HRTEM image of the heterojunction with a 9 nm-thick $PtSe_2$. EDS mapping: (b) Pt, (c) Se.

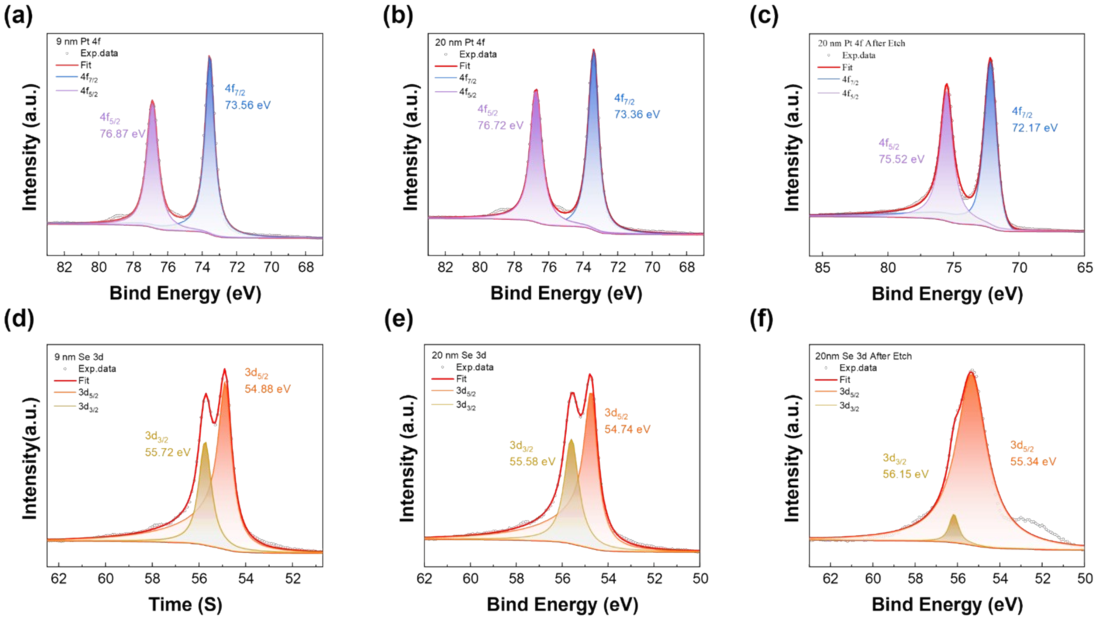

Figure S5. The XPS spectra of $PtSe_2$ with varying thicknesses. The Pt 4f core level: (a) 9 nm $PtSe_2$, (b) 20 nm $PtSe_2$, (c) 20 nm $PtSe_2$ after etching 12 nm. The Se 3d core level: (d) 9 nm $PtSe_2$, (e) 20 nm $PtSe_2$, (f) 20 nm $PtSe_2$ after etching 12 nm. The 9 nm-thick $PtSe_2$ film was fully selenized. The surface of the 20 nm-thick $PtSe_2$ was fully selenized, but within the interior (i.e. 12 nm depth), incomplete selenization was evident. This is indicated by the shifted peaks of the Pt core level and the changes in the profile of the Se core level.

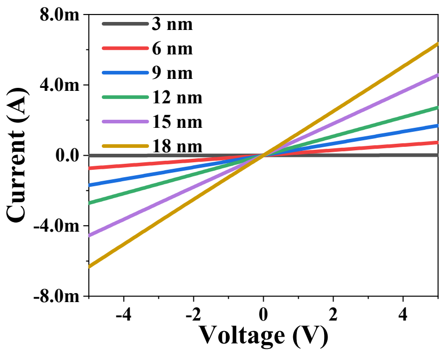

Figure S6. IV curves of the $PtSe_2$ films with various thicknesses.

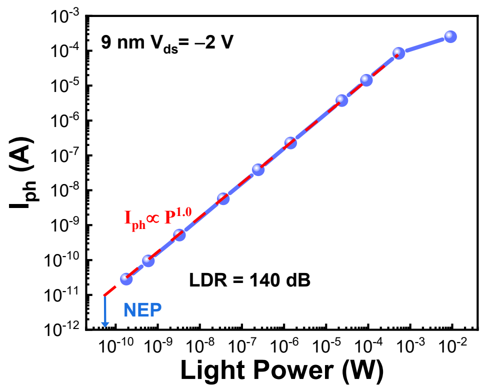

Figure S7. Photocurrent versus light power at 520 nm under −2 V bias.

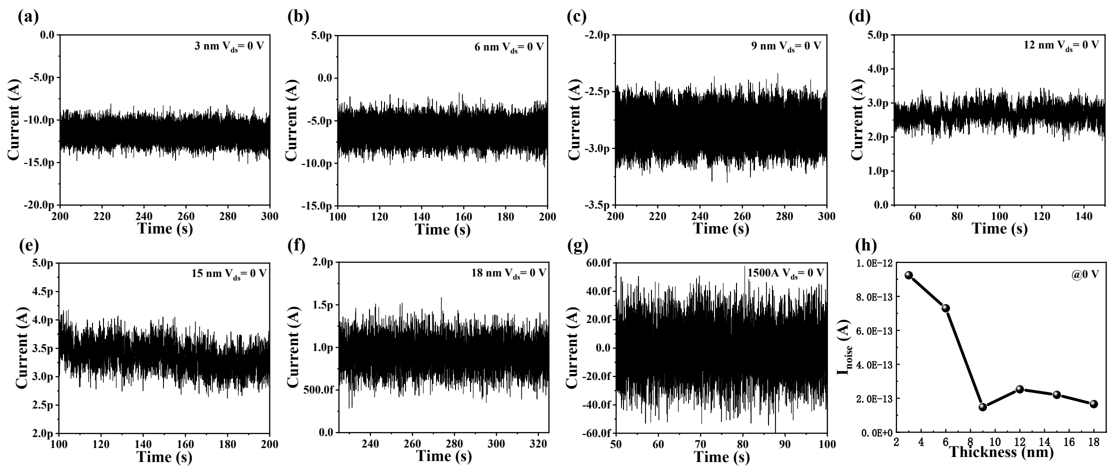

Figure S8. Dark-state current as a function of time under 0 V bias. (a) 3 nm, (b) 6 nm, (c) 9 nm, (d) 12 nm, (e) 15 nm, (f) 18 nm, (g) without device, (h) root-mean-square noise current as a function of $PtSe_2$ film thickness. The none zero average currents are originated from the zero drift or offset from the source-and-measurement unit.

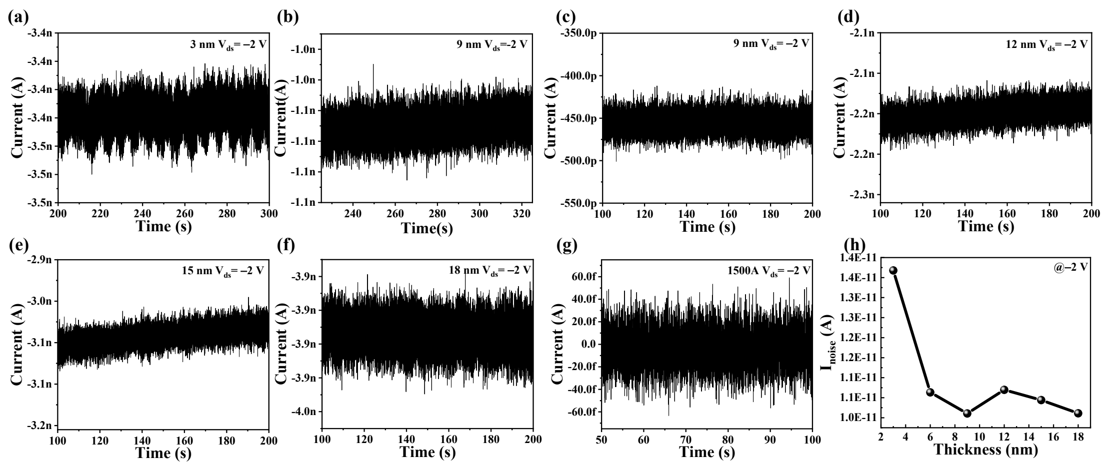

Figure S9. Dark-state current as a function of time under −2 V bias. (a) 3 nm, (b) 6 nm, (c) 9 nm, (d) 12 nm, (e) 15 nm, (f) 18 nm, (g) without device, (h) root-mean-square noise current as a function of $PtSe_2$ film thickness.

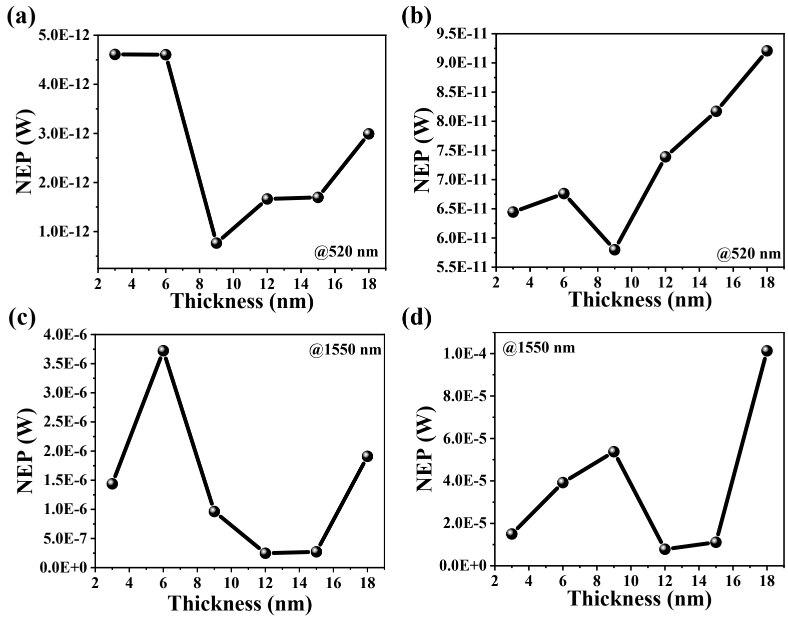

Figure S10. NEP as a function of $PtSe_2$ film thickness. 520 nm: (a) 0 V, (b) −2 V. 1550 nm: (c) 0 V, (d) −2 V.

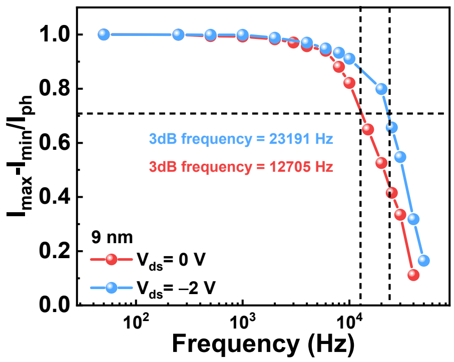

Figure S11. 3dB bandwidths at 520 nm under 0 V and −2 V biases.

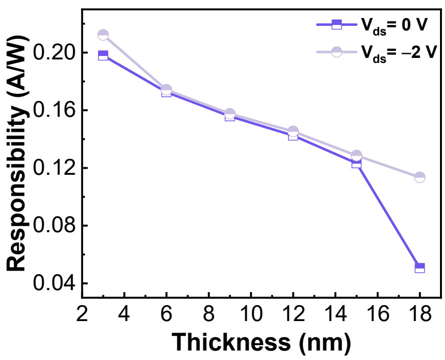

Figure S12. Responsivities versus $PtSe_2$ film thickness at 520 nm under 0 V and −2 V biases.

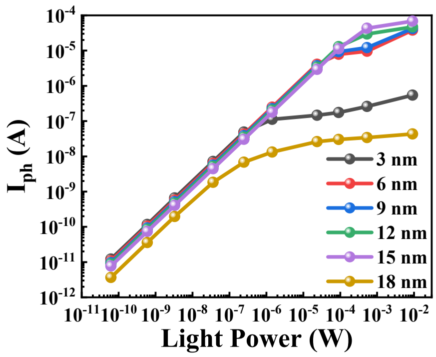

Figure S13. photocurrent versus light power at 520 nm under 0 V bias.

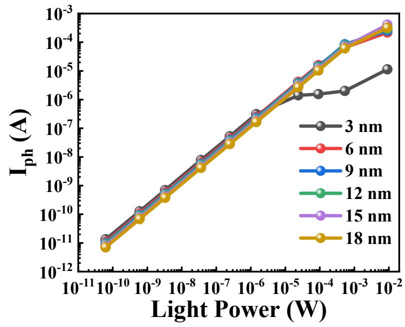

Figure S14. Photocurrent versus light power at 520 nm under −2 V bias.

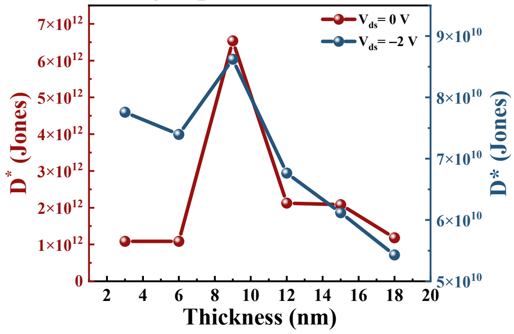

Figure S15. Specific detectivity (D*) of the devices with varying $PtSe_2$ thickness at 520 nm under 0 V and −2 V biases.

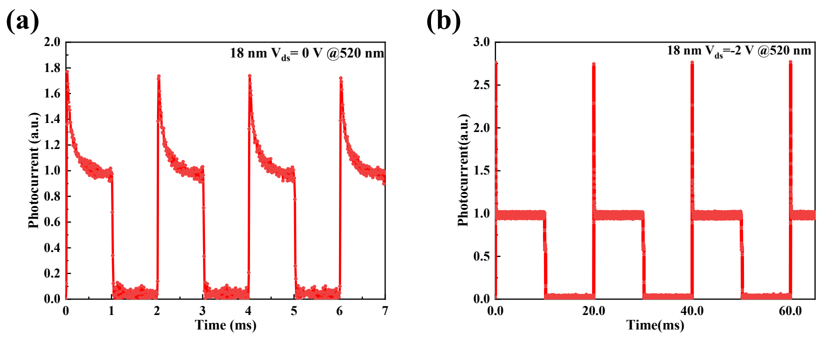

Figure S16. Current-time of the device with an 18 nm thick $PtSe_2$ layer under rectangular pulsed light illumination. (a) 0 V (b) −2 V.

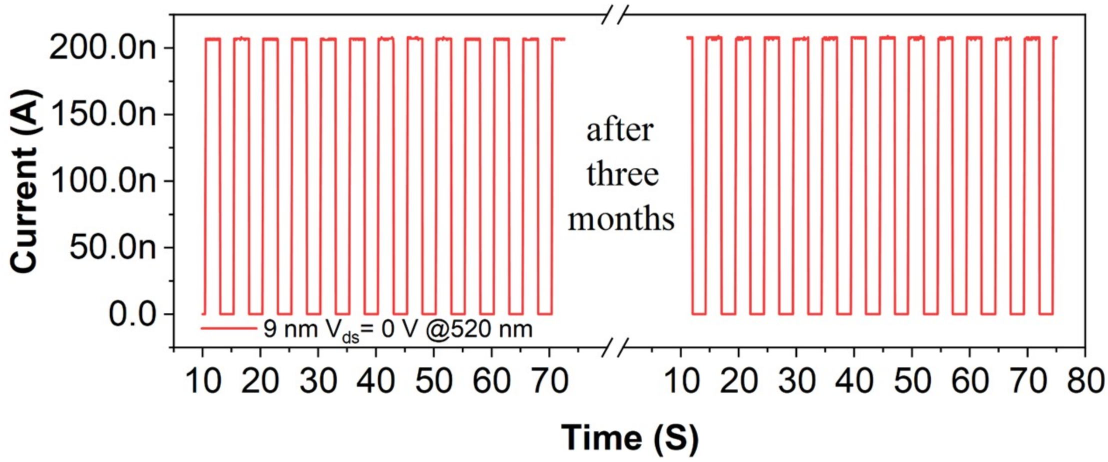

Figure S17. Temporal response of the photodetector under the light illumination with alternating on and off cycles.

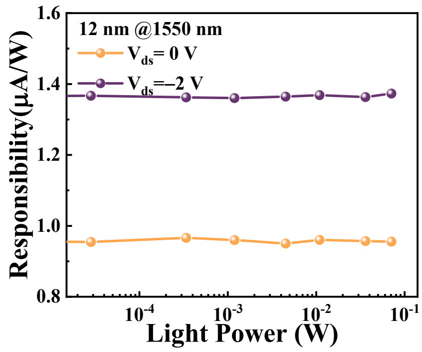

Figure S18. Responsivities as a function of light power for device with 12 nm thick $PtSe_2$ under 0 V and −2 V biases.

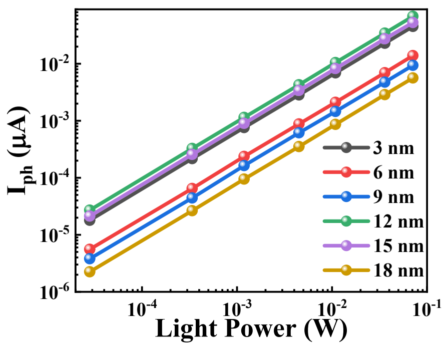

Figure S19. Photocurrent versus light power at 1550 nm under 0 V bias.

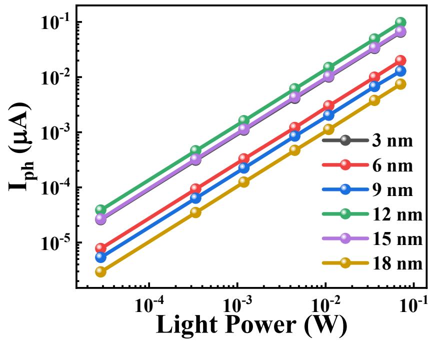

Figure S20. Photocurrent versus light power under −2 V bias.

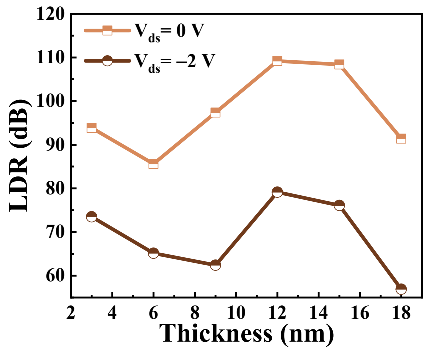

Figure S21. LDRs as a function of $PtSe_2$ layer thickness at 1550 nm under 0 V and −2 V biases.

Table S1. Photodetection performance comparison

Devices	Wavelength (nm)	Bias (V)	*R* (A/W)	LDR (dB)	*D** (Jones)	Response time (μs)	Ref.
$PtSe_2$ (9 nm)-Si	520	0	0.16	157	6.5×10^{12}	78	Our work
		−2	0.16	139	8.6×10^{10}	38	
	800	0	0.24	-	9.1×10^{12}	-	
$PtSe_2$ (3 nm)-Si	950	0	0.44	-	2.4×10^{12}	-	
		−2	0.49	-	1.7×10^{11}	-	
$PtSe_2$-Si pin	532	−2	0.054	58	1.35×10^{11}	2.2/11.8	[2]
$PtSe_2$-Si	808	0	0.52	114	3.26×10^{13}	55/170	[3]
$PtSe_2$-Si nanowire array	780	−5	12.65	92	2.5×10^{13}	10.1/19.5	[4]
$PtSe_2/Bi_2Te_3$/pyramid Si	980	0	0.62	100	1.37×10^{12}	0.45/18	[5]
Graphene/PtSe2/Pyramid Si	980	0	0.528	~80	4.36×10^{12}	8.5/10.2	[6]
PtSe2/ultrathin SiO2/Si	808	0	8	158	4.78×10^{13}	14.1/15.4-	[7]
$PtSe_2$/graphene/Si	808	−1	0.81	-	1.29×10^{9}	43.6/51.2	[8]
$PtSe_2$/i-Si/n-Si	532	0	0.0465	-	1.94×10^{11}	-	[9]
		−2	0.05	78	4.78×10^{9}	70/290	

Table S2. Performance parameters of the $PtSe_2$-Si heterojunction photodetectors at 532 nm.

$PtSe_2$ thickness (nm)	Bias (V)	*R* (A/W)	*D** (Jones)	LDR (dB)	Response times (μs)
3	0	0.198	1.08×10^{12}	95	92
	−2	0.212	7.76×10^{10}	123	62
6	0	0.172	1.09×10^{12}	134	84
	−2	0.174	7.39×10^{10}	122	45
9	0	0.155	6.53×10^{12}	157	78
	−2	0.157	8.62×0^{10}	139	38
12	0	0.142	2.12×10^{12}	155	86
	−2	0.145	6.76×10^{10}	137	43
15	0	0.123	2.08×10^{12}	155	1110
	−2	0.128	6.12×10^{10}	136	109
18	0	0.051	1.18×10^{12}	61	-
	−2	0.113	5.43×10^{10}	135	-

Table S3. Performance parameters of the $PtSe_2$-Si heterojunction photodetectors at 1550 nm.

$PtSe_2$ thickness (nm)	Bias (V)	*R* (μA/W)	*D** (Jones)	LDR (dB)	Response times (ms)
3	0	0.63	3.46×10^{6}	95	5.56
	−2	0.91	3.34×10^{5}	123	1.31
6	0	0.20	1.34×10^{6}	134	3.79
	−2	0.27	1.28×10^{5}	123	0.32
9	0	0.14	5.20×10^{6}	157	0.46
	−2	0.19	9.29×10^{4}	139	0.41
12	0	0.95	1.43×10^{7}	155	0.52
	−2	1.36	6.38×10^{5}	137	0.47
15	0	0.76	1.31×10^{7}	155	1.96
	−2	0.96	4.50×10^{5}	136	1.84
18	0	0.08	1.85×10^{6}	61	-
	−2	0.10	4.94×10^{4}	135	-

References

1. S. Cheung and N. Cheung, *Applied Physics Letters*, 1986, **49**, 85-87.
2. T. Ji, S. Ke, X. Xu, S. Chen, Z. Li, Z. Huang, G. Liu, J. Zhou, Z. Wang and C. Wang, *ACS Photonics*, 2024, **11**, 3150-3159.
3. C. Xie, L. Zeng, Z. Zhang, Y.-H. Tsang, L. Luo and J.-H. Lee, *Nanoscale*, 2018, **10**, 15285-15293.
4. L. Zeng, S. Lin, Z. Lou, H. Yuan, H. Long, Y. Li, W. Lu, S. P. Lau, D. Wu and Y. H. Tsang, *NPG Asia Materials*, 2018, **10**, 352-362.
5. X. Li, K. Liu, R. Zhuo, L. Zeng, P. Lin, L. Li, Z. Shi, Y. Tian, X. Li and D. Wu, *ACS Photonics*, 2024, **11**, 2070-2076.
6. L. Zeng, W. Han, S.-E. Wu, D. Wu, S. P. Lau and Y. H. Tsang, *IEEE Transactions on Electron Devices*, 2022, **69**, 6212-6216.
7. P. Ye, H. Xiao, Q. Zhu, Y. Kong, Y. Tang and M. Xu, *Science China Materials*, 2023, **66**, 193-201.
8. Q. Zhu, S. Wei, J. Sun, Y. Sun and M. Xu, *Nanoscale*, 2024, **16**, 19865-19872.
9. X. Xu, S. Ke, T. Ji, M. Ge, Z. Li, Y. Chen, B. Liu, Z. Huang, J. Zhou and G. Liu, *ACS Applied Materials & Interfaces*, 2025,**17**,15579-15592